A discriminating microscopy technique for the measurement of ice crystals and air bubbles size distribution in sorbets

O. Hernandez, F. Ndoye, H. Benkhelifa, D. Flick, G. Alvarez

ID:573

A DISCRIMINATING MICROSCOPY TECHNIQUE FOR THE MEASUREMENT OF ICE CRYSTALS AND AIR BUBBLES SIZE DISTRIBUTION IN SORBETS

Oscar HERNANDEZ[(*,,***)], Fatou NDOYE[(*)], Hayat BENKHELIFA[(**,***)], Denis FLICK[(**,***)], Graciela ALVAREZ [(*)]**

[(*)]IRSTEA, 1 rue Pierre Gilles de Gennes, Antony, F-92761, France
[(**)]AgroParisTech, UMR1145 Ingénierie Procédés Aliments, F-75005 Paris, France
[(***)] INRA, UMR1145 Ingénierie Procédés Aliments, F-91300 Massy, France

ABSTRACT

In this work, a technique capable to distinguish between ice crystals and air bubbles in sorbets was developed in order to characterize the effect of operating conditions on their size distributions at the exit of the freezer. A pilot freezer was used to crystallize and aerate a commercial lemon sorbet mix. Crystals and bubbles sizes were measured using a light microscope technique under low temperature in a refrigerated glove box developed in the lab for that purpose. Results showed that the developed microscope technique allowed to distinguish them and to quantify their size distributions. Measurements showed that ice crystals size decreases with air flow rate while air bubbles size increases. The latter also increases with the cylinder pressure inside the scraped surface heat exchanger (SSHE).

1. INTRODUCTION

Sorbets are frozen desserts made by freezing of a formulated liquid mix similar to ice creams. However, sorbets differ from ice creams in the absence of fat and the replacement of dairy ingredients for fruit or fruit juices. Sorbets contain at least 25% frozen fruit and/or fruit juice, a high sugar concentration, and may be stabilized with egg whites, pectin, or gum stabilizers. From a structural point of view, sorbets are comprised of different phases arranged in a complex way that encompasses different size scales. On a microscopic scale it is possible to differentiate three main phases: solid ice crystals, a serum liquid phase, and dispersed air bubbles.

The manufacture of sorbets and ice creams is commonly carried out using scraped surface heat exchangers (SSHEs) in ensembles called freezers. The water present in the liquid phase is crystallized on the walls of the exchanger; the ice is scraped away from them and broken forming numerous ice crystals of different sizes. Also, air is incorporated into the sorbet mix by whipping the air flow with the scrapers, forming bubbles of different sizes, and dispersing them into the mixture of liquid and ice crystals. The state of this dispersion, and particularly the size distributions obtained, are strongly dependent on operating conditions inside the SSHE such as the rotation speed of the scraper blades or the air flowrate used (e.g. Cook and Hartel (2011, Chang and Hartel (2002)). Additionally it has been shown how the state of this dispersion may influence the sensory perception by consumers (e.g. Warren and Hartel (2014)). Therefore, a simultaneous monitoring and control of the size distributions of both, ice crystals and air bubbles, is important in order to optimize and control the crystallization-foaming process and the induced product functionalities.

Several methods have been purposed for measurement of crystal sizes and bubble sizes in ice creams. One of the first and most commonly used is the use of an optical microscope in a cold room (e.g. Donhowe *et al.* (1991), Chang and Hartel (2002)), with the help of special lighting (e.g. episcopic coaxial lighting (Faydi *et al.* (2001), Caillet *et al.* (2003)), or fluorescence (e.g. Regand and Goff (2003)), scanning (e.g. Miller-Livney and Hartel (1997), Russell *et al.* (1999)) or transmission electron microscopy (e.g. Goff *et al.* (1999)). Most of these methods are not suitable to online measurement because they require special characteristics in order to be carried out (e.g. immersion in liquid nitrogen Woinet *et al.* (1998) or the use of solvents for obtaining one or the other distribution) that can alter or destroy the structure of the ice cream sample. Recently, focused beam reflectance methods (FBRM) have been used to measure the crystal size distribution (CSD) online during non-aerated sorbet production (Arellano *et al.* (2012)), and study of recrystallization

phenomena during storage of ice creams (Ndoye and Alvarez (2015)) and for measurement of micro bubbles during fermentation (Druzinec *et al.* (2015)). However our preliminary experiments in aerated sorbets showed that, with both phases present, FBRM failed to discriminate between both distributions, since, due to the reflective nature of the method, it casts doubt on whether any chord length measured correspond to an entire ice crystal, an entire bubble, or an interface thickness on any object.

The purpose of this work was to develop a granulometric method able to distinguish between ice crystals and air bubbles in order to evaluate the effect of operating conditions on their size distributions in aerated sorbets produced in SSHEs, aiming to disrupt the least possible the internal structure of the samples unlike all methods cited above. The application of this technique will mainly involve samples obtained at the exit of the SSHE. For that matter, crystals and bubbles sizes in aerated sorbets were measured using a light microscope technique under low temperature in a refrigerated glove box developed in the lab for that purpose.

2. MATERIALS AND METHODS

2.1 Lemon sorbet mix and commercial sorbets

A commercial ultra-high temperature pasteurized lemon sorbet mix (14.6% w/w sucrose, 8% w/w fructose, 0.09% w/w dextrose, 3% w/w lemon juice concentrate 60 Brix, 0.5% w/w locust bean gum/guar gum/ hypromellose stabiliser blend) obtained from Laiterie de Montaigu (Montaigu, France) was used in this work for sorbet production.

2.2 Freezing of the sorbet mix

Freezing of the mix was carried out in a laboratory scale continuous pilot freezer (WCB® Model MF 50) represented in Figure 1. The mix to be frozen was stored in a reservoir of 200 L capacity connected through a jacket to a thermostatic bath in order to keep a constant inlet temperature, which was monitored using calibrated type-T thermocouples. Mix was allowed to cool down to 3°C for approx. 1 h before being pumped into the freezer by a piston pump at a controlled rate of 25 kg/h. Within the freezer, the air was introduced to the mix flow through a non-return valve in a T-joint before the entrance to the SSHE. The air flowrate is given here in terms of volumetric flowrate at 15°C and 5,5 bar. It was regulated manually (0 - 43 L/h) using a Brooks GT1350 rotameter (Hatfield PA, USA) and corrected according to its temperature (measured by a Type-T thermocouple) and pressure (measured using a Baumer® sensor) during operation.

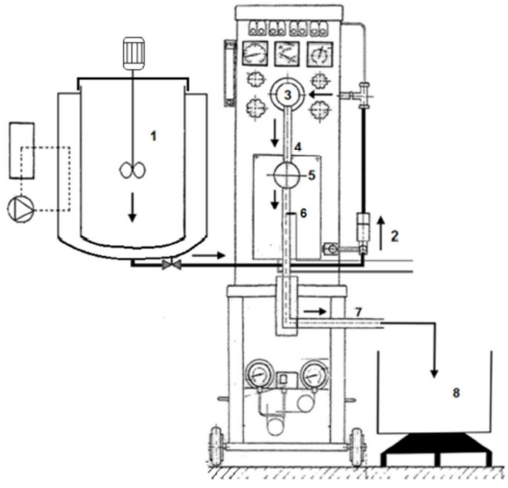

Figure 1. Schematic representation of the freezer used in this work. 1. Refrigerated jacketed feed tank, 2. Mix pump, 3. Scraped surface heat exchanger, 4. Sorbet exit pipe, 5. Membrane valve, 6. Draw temperature thermocouple, 7. Product sampling point, 8. Disposal reservoir

The SSHE within the freezer consists of a jacketed cylinder (0.05 m inner diameter, 0.40 m long) which contains a solid rotor equipped with two scraper blades. The rotor occupied approximately 46% of the freezer barrel volume. The total volume of the SSHE available to the working fluid was 0,67 L, which includes the volume available within the heat exchange cylinder, the inlet and outlet bowls, as well as the outlet pipe. The outlet pipe of the SSHE represents 20% of the total available volume to the fluid. The heat

exchange surface of the SSHE was cooled by refrigerant fluid R22 evaporating at -15°C in the external jacket. A calibrated type-T thermocouple with an accuracy of ±0.2°C was fixed with conductive aluminum tape on the external surface wall of the cooling jacket, so as to measure the evaporation temperature of the refrigerant fluid. An indirect control of this temperature was allowed by manipulation of the pressure on the compressor attached to the refrigeration cycle within the freezer. The dasher rotational speed was measured by means of a photoelectric tachometer (Ahlborn®, type FUA9192) with an accuracy of 1 rpm. The control of the rotation speed of the dasher, the compressor drive rotation speed and the mix flow rate are carried out using three AC Drives (Series 650 Parker®) connected to the dasher, refrigeration cycle compressor and mix pump. The accuracy of the mix flowrate control was determined to be ± 0,33 kg h^{-1}. The draw temperature of the product was measured online by means of a calibrated Pt100 probe (Baumer®, accuracy of ±0.1 °C). The Pt100 probe was inserted into the outlet pipe of the SSHE before the exit of the product. The pressure inside the SSHE was adjusted manually by action of a membrane valve placed at the exit of the SSHE.

Programs written on LabVIEW® allowed control of variables and collected all operating conditions by means of two data acquisition units Agilent HP (Model 34970 A) and two Switch Units Agilent HP (Model 34901 A) connected to a PC. The acquisition of data is performed every 5 s.

When the operation of the freezer started and the desired operating conditions were set up, the freezer was allowed to achieve steady-state operation for approx. 30 min before recovering the product. The steady-state was checked visually from plots of the history of the variables observed (temperatures and pressures). The samples were recovered at the exit using carton boxes of 250 mL by carefully filling them and covering them with a lid. According to the measurement required, some of them were stored at -30°C and some used immediately for analysis. For all analysis carried out, the samples were collected by triplicate.

2.3 Low-temperature light microscopy analysis

For microscopy observation, a light microscope (OMAX) with a camera connection to computer was used. Since sorbet samples are highly sensitive to temperature (i.e. melting of the ice crystals, coalescence of bubbles, etc.) a refrigerated glove box inspired in the work by Donhowe *et al.* (1991) was built adapting a double-door domestic freezer cabinet as shown in Figure 2a. The cabinet was divided by a wall creating a circuit of air flow blown using a fan. A refrigeration system on top and an electrical heater installed on the bottom were used to set up a control on the temperature in the workspace within a range of -25 to +25°C ± 1°C. Also, a shelf was installed above the workspace where a bed of silica-gel beads ensure low moisture content in the circulating air in order to avoid frosting in the lenses of the microscope or the cabinet.

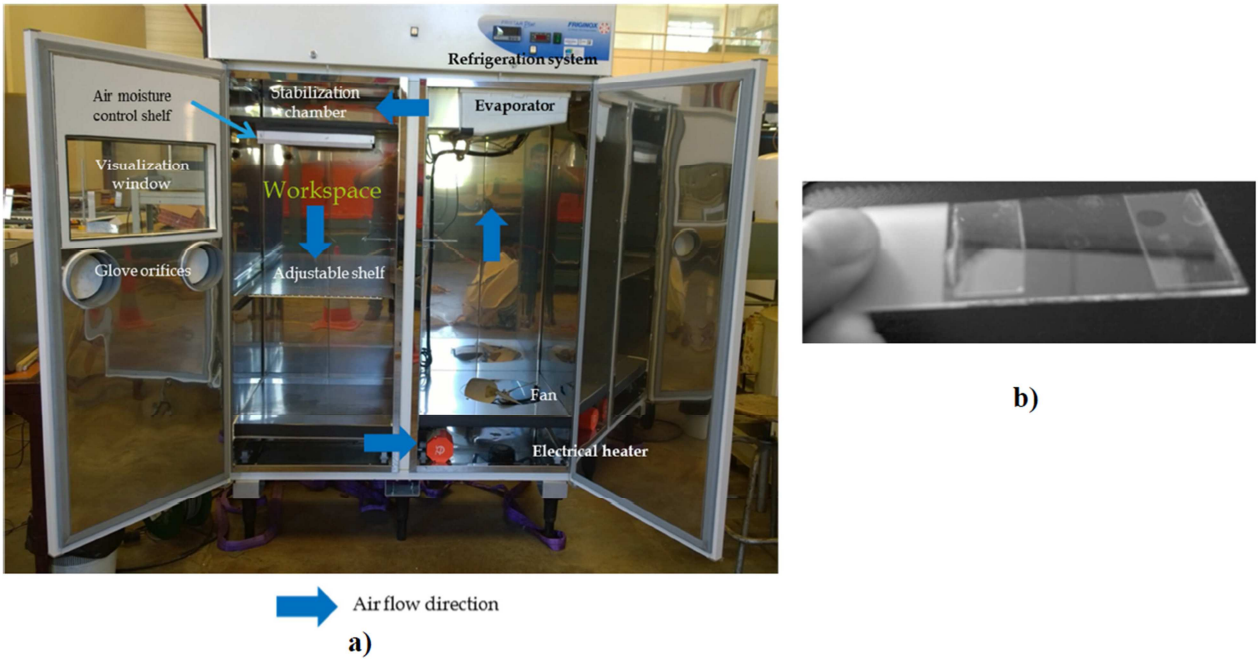

Figure 2. Experimental equipment and tools required for the low-temperature light microscopy observation of crystals and bubbles in aerated sorbets: a) Refrigerated glove box built for this work, b) Microscope slides used in this work.

All necessary equipment for the microscope observation (slips, slides, microscope, sample, spatulas, etc.) was placed within the refrigerated glove box at -10°C and allowed to cool down before any measurement. The slides used regularly in microscope observations were modified as shown in Figure 2b. A pair of pieces of slips was glued carefully at both extremes of the slide providing a support for the covering slip to be placed. This also left a space with a thickness of approximately 240 µm between the covering slips and the slides.

The carton boxes containing the recovered sorbet were introduced into the glove box for analysis. Immediately, samples from the sorbet were extracted from the center of the carton using a small spatula. Typically, the amount recovered by the spatulas did not exceed 10 mg. They were placed in the space between the slip supports carefully while gently allowing them to spread throughout the space. Once the samples were spread, they were cover by a slip and placed under observation. Several pictures on different random zones on the visualization field were taken and used for image analysis.

Image analysis was carried out using the software ImageJ®. Using a picture from a calibrated scale in a slide it was obtained the number of pixels that accounted for a known length. With this scale then it was possible to measure different bubbles and crystals for characterization. Since bubbles are mostly spherical, a line approximating at best each diameter was drawn on the bubble and the length of those lines provided the diameters of the bubbles. This information was saved for further analysis. For the crystals, since they have irregular shapes, a polygon approximating their observed shape was drawn on them. Using the polygon, the software calculated the projected surface area, perimeter, circularity and the maximal Feret diameter (i.e. the longest distance between the vertices of the polygon) for each crystal and the information for all of them was registered for further analysis. Typically, more than 200 bubbles or crystals were registered from all the pictures in every condition. For CSD, the maximal Feret diameter, the projected area-based diameter (i.e. the diameter of a circle with an area equal to the polygon area) and a perimeter-based diameter (i.e. the diameter of a circle with a perimeter equal to the polygon perimeter) were used to represent the CSD function. For bubble size distributions (BSD) and CSDs, bins of 10 µm width were used for estimating the frequencies of the distributions. A typical example of application of this technique is presented in Figure 3. The standard deviation of the bubble and crystal mean sizes observed using this technique were typically less than 2 µm.

3. RESULTS AND DISCUSSION

3.1 Observations with low-temperature light microscopy technique

For samples obtained when the operating conditions were set as 25 kg/h of mix flowrate, refrigerant temperature of -15°C, and 300 rpm of dasher speed, the low temperature light microscopy technique was applied. The air flowrates and SSHE pressures were varied from 0 to 43 L/h and 2,5 to 5,0 bar, respectively. The results are summarized in Figure 4 and Figure 5. It is noteworthy that the values observed for mean sizes are within the range previously reported as common for ice crystals produced in SSHEs (Cook and Hartel (2011)). It can be noticed from the example of the CSD in Figure 3b that even if different forms of the CSD are obtained, they were not very different. This was expected since the circularity on all samples was usually above 0,8 (data not shown here). However, since the images are a two-dimensional perspective it is impossible to relate this value with the real shape of the observed ice crystals, while techniques such as episcopal lighting microscopy can offer such comparison. The high circularity also shows that an analysis based on any of the diameters established in this work are suitable to represent CSDs.

3.2 Effect of operating conditions observed on BSD and CSD observed using the microscopy technique

For evaluating how operating conditions are reflected in the measurement with the low-temperature microscopy technique, sorbet mix was frozen varying the SSHE pressure and the air volume flowrate while keeping the mix flowrate at 25 kg/h, the R22 evaporating temperature at -15°C and the dasher speed at 300 rpm. The effect is presented in Figure 4 using the maximal Feret diameter as representation of the CSD. The mean crystal size seems to decrease with an increase in the air flowrate. This observation agrees with those presented by Sofjan and Hartel (2004) for ice creams and could be explained by an insulating effect of air in the heat transfer throughout the heat exchanger, and a possible physical obstruction which impedes ice crystal growth. On the other hand, the pressure in the SSHE seemed to have almost no effect on the observed crystal size

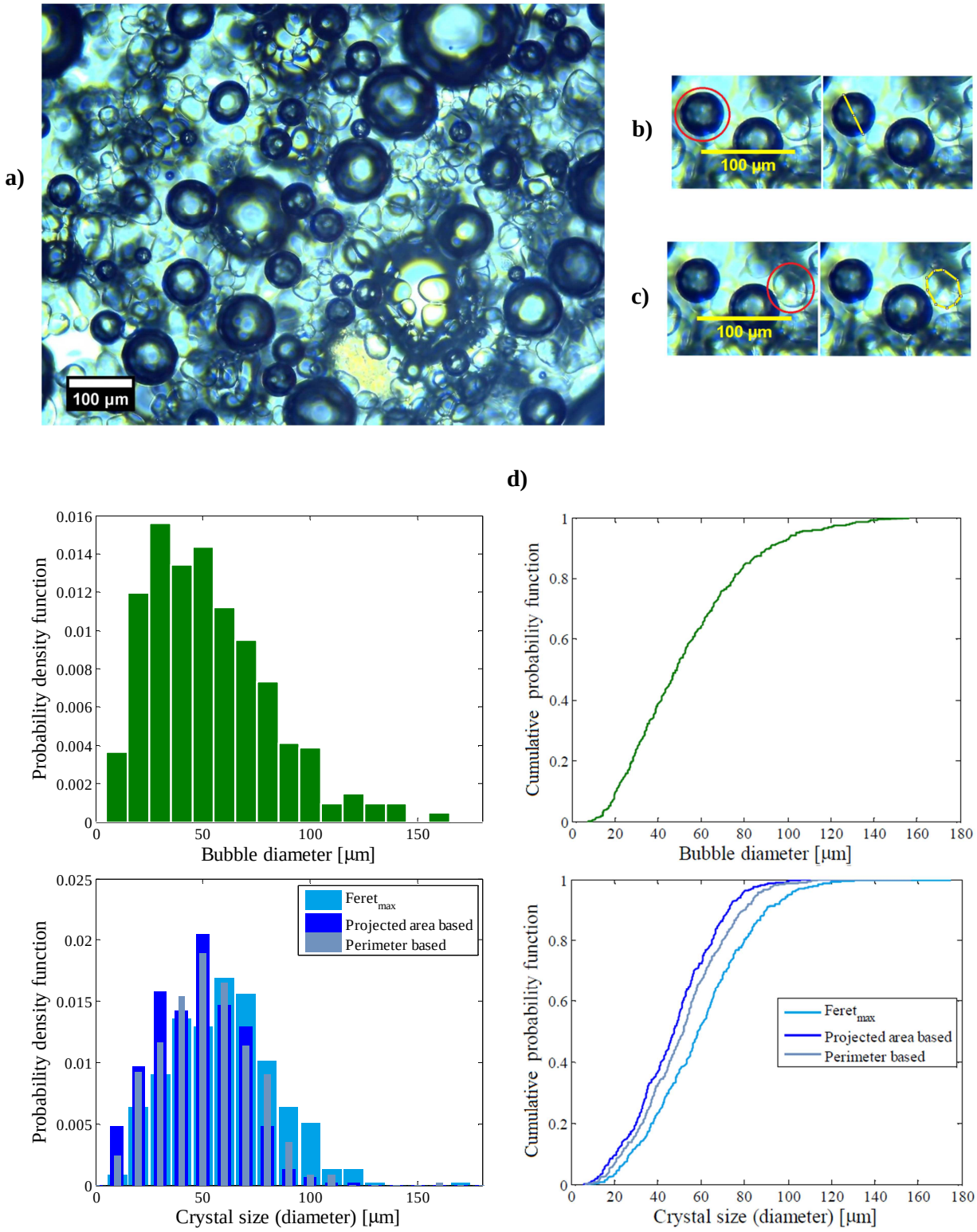

Figure 3. Example of analysis of lemon sorbet samples with the low-temperature light microscopy technique developed in this work. The observation was carried out immediately after production. Operating conditions were set up as 25 kg/h of mix flowrate, R22 evaporating temperature of -15°C, dasher speed of 750 rpm and air volume flowrate of 10,1 L/h. a) Raw images, b) bubble measurement, c) crystal measurement, and d) BSD (green) and CSDs plots typically obtained (blue, see the legend in the figures for more details)

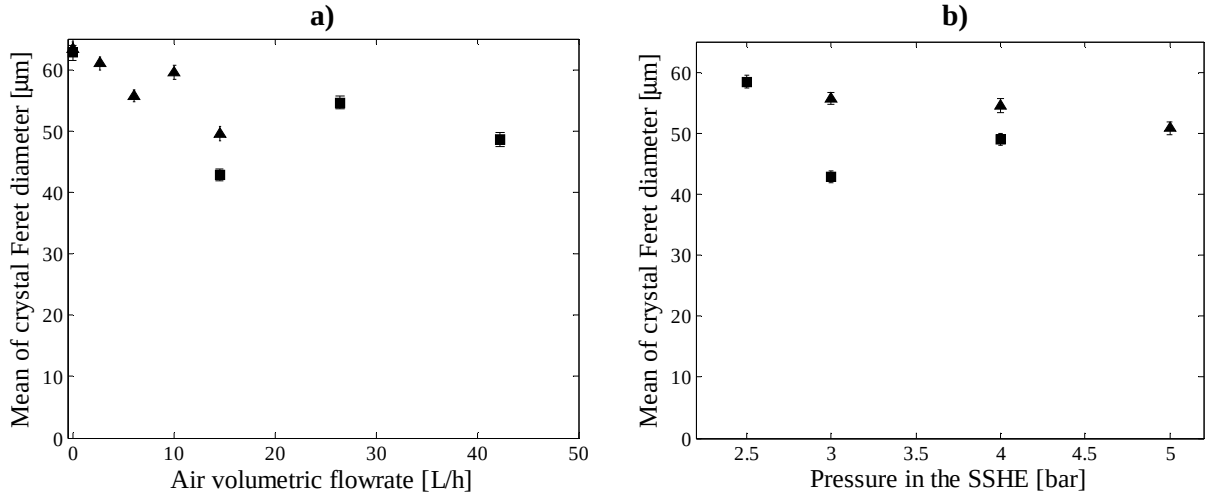

Figure 4. Effect of operating conditions on the CSD represented by the maximal Feret diameter. a) Effect of air flowrate on the mean crystal size (pressure inside the SSHE kept constant as 4 bar) when the sample were analyzed immediately after production (■) and analyzed after storage for 24 h at -30°C (▲), b) Effect of the SSHE internal pressure on the mean crystal size when the samples were analyzed immediately after production at air volume flowrate of 7 L/h (▲) and 15 L/h (■)

The effect of air flowrate and SSHE pressure on the measured BSD is shown in Figure 5. The results obtained are in the range expected for air cell bubbles in ice creams produced in freezers (e.g. Eisner *et al.* (2005), Chang and Hartel (2002)) even if no fat matter or milk proteins are present in this case. Mean bubble diameters obtained increased with air flowrate, probably due to the fact that a larger air flowrate implies a larger amount of bubbles present in the sample during the structuring of the product increasing the coalescence between them and giving rise to a larger bubble mean diameter. Also, it is remarkable that these results are qualitatively similar to those presented by Müller-Fischer and Windhab (2005) for continuous foaming in toothed rotor-stator devices, however the mean bubble diameters presented in this paper are smaller, probably due to the difference in operating conditions and the presence of milk proteins and fat matter that establish a different dynamics on the stabilization of bubbles dispersed in the liquid.

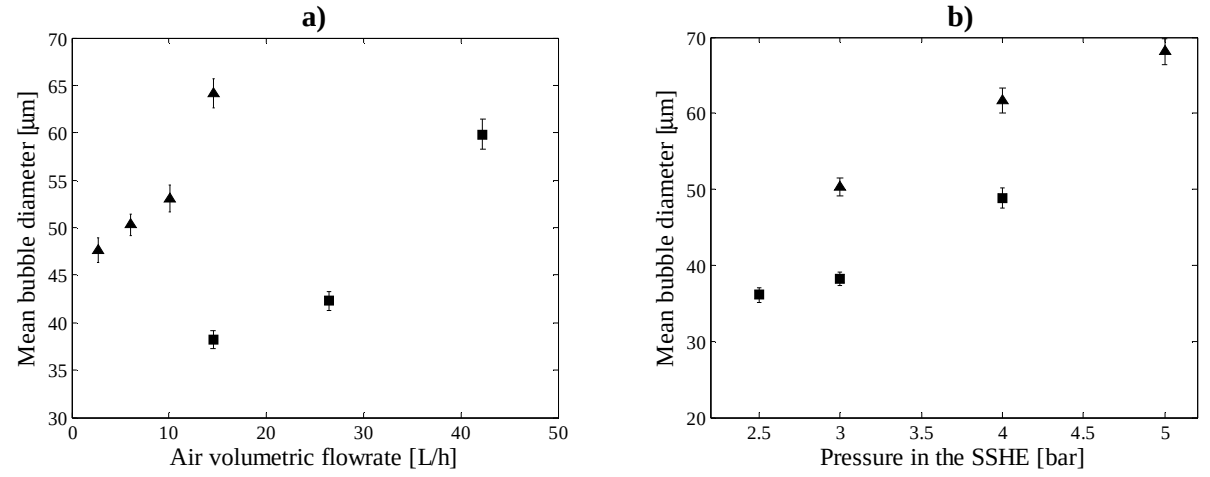

Figure 5. Effect of operating conditions on the BSD. a) Effect of air flowrate on the mean diameter when the sample were analyzed immediately after production (▲) and analyzed after storage for 24 h at -30°C (■), b) Effect of the SSHE internal pressure on the mean crystal size when the samples were analyzed immediately after production at air volume flowrates of 7 L/h (▲) and 15 L/h (■)

The effect of the pressure inside the SSHE on the mean bubble diameter is depicted in Figure 5b. At different air flow rates, the mean bubble diameter seems to increase linearly with pressure in the range of this study. A similar trend was observed by Müller-Fischer and Windhab (2005) in toothed rotor-stator devices, however the pressure range covered by that work was lower (between 0 and 2 bar). This trend could be explained by

the fact that the bubbles undergo a higher volume expansion at the outlet of the freezer when the pressure within is higher.

4. CONCLUSIONS

Results showed that the low temperature microscope technique developed in this work allowed the discrimination and quantification of the BSD and CSD of aerated sorbets while preserving a good vision of the internal microscopic structure of the samples. The values obtained for both distributions using this technique were in the range of previous published data which attest its suitability for such measurement.

Measurements showed that ice crystals size decreases with air flow rate while air bubbles size increases. The latter also increases with the cylinder pressure inside the SSHE. The crystals obtained showed a rather circular projected area, and therefore, CSD based on maximal Feret diameter, projected area or perimeter can represent equally well the distribution.

5. REFERENCES

Cook KLK and Hartel RW 2011, Effect of freezing temperature and warming rate on dendrite break-up when freezing ice cream mix, *International Dairy Journal* 21(6): 447-453

Chang Y and Hartel RW 2002, Measurement of air cell distributions in dairy foams, *International Dairy Journal* 12(5): 463-472

Warren MM and Hartel RW 2014, Structural, Compositional, and Sensorial Properties of United States Commercial Ice Cream Products, *Journal of Food Science* 79(10): E2005-E2013

Donhowe DP *et al.* 1991, Determination of Ice Crystal Size Distributions in Frozen Desserts, *Journal of Dairy Science* 74(10): 3334-3344

Faydi E *et al.* 2001, Experimental study and modelling of the ice crystal morphology of model standard ice cream. Part I: Direct characterization method and experimental data, *Journal of Food Engineering* 48(4): 283-291

Caillet A *et al.* 2003, Characterization of ice cream structure by direct optical microscopy. Influence of freezing parameters, *LWT - Food Science and Technology* 36(8): 743-749

Regand A and Goff HD 2003, Structure and ice recrystallization in frozen stabilized ice cream model systems, *Food Hydrocolloids* 17(1): 95-102

Miller-Livney T and Hartel RW 1997, Ice Recrystallization in Ice Cream: Interactions Between Sweeteners and Stabilizers, *Journal of Dairy Science* 80(3): 447-456

Russell AB *et al.* 1999, Influence of freezing conditions on ice crystallisation in ice cream, *Journal of Food Engineering* 39(2): 179-191

Goff HD *et al.* 1999, A study of fat and air structures in ice cream, *International Dairy Journal* 9(11): 817-829

Woinet B *et al.* 1998, Experimental and theoretical study of model food freezing. Part II. Characterization and modelling of the ice crystal size, *Journal of Food Engineering* 35(4): 395-407

Arellano M *et al.* 2012, Online ice crystal size measurements during sorbet freezing by means of the focused beam reflectance measurement (FBRM) technology. Influence of operating conditions, *Journal of Food Engineering* 113(2): 351-359

Ndoye FT and Alvarez G 2015, Characterization of ice recrystallization in ice cream during storage using the focused beam reflectance measurement, *Journal of Food Engineering* 148(0): 24-34

Druzinec D *et al.* 2015, Micro-bubble aeration in turbulent stirred bioreactors: Coalescence behavior in Pluronic F68 containing cell culture media, *Chemical Engineering Science* 126(0): 160-168

Sofjan RP and Hartel RW 2004, Effects of overrun on structural and physical characteristics of ice cream, *International Dairy Journal* 14(3): 255-262

Eisner MD *et al.* 2005, Air cell microstructuring in a high viscous ice cream matrix, *Colloids and Surfaces A: Physicochemical and Engineering Aspects* 263(1–3): 390-399

Müller-Fischer N and Windhab EJ 2005, Influence of process parameters on microstructure of food foam whipped in a rotor–stator device within a wide static pressure range, *Colloids and Surfaces A: Physicochemical and Engineering Aspects* 263(1–3): 353-362